Closed-form solutions for thermomechanical buckling of orthotropic composite plates

Gutiérrez Álvarez, Javier; Bisagni, Chiara

DOI
10.1016/j.compstruct.2019.111622

Publication date
2020

Document Version
Final published version

Published in
Composite Structures

Composite Structures 233 (2020) 111622

Contents lists available at ScienceDirect

Composite Structures

journal homepage: www.elsevier.com/locate/compstruct

Closed-form solutions for thermomechanical buckling of orthotropic composite plates

Javier Gutiérrez Álvarez*, Chiara Bisagni

Aerospace Structures and Computational Mechanics, Faculty of Aerospace Engineering, Delft University of Technology, Delft, The Netherlands

ARTICLE INFO

Keywords:
Thermomechanical buckling
Closed formula
Thermal stresses
Preliminar design

ABSTRACT

A closed-form solution is derived for the buckling of orthotropic composite plates under the effect of thermal and mechanical loads. The plates are subjected to constant temperature increment and length variation while the width expansion is constrained. The problem is formulated in terms of displacement components, studied using classical plate theory in combination with classical lamination theory. An analytical formula that relates critical temperatures to applied plate displacements is obtained. The buckling of heated, fully restrained plates is also derived as a particular case. Examples of plates made of different materials and lay-ups are presented in graphical form, and are verified by finite element analysis. The obtained formula can be used during initial design, for sensitivity analysis and also for obtaining desired buckling shapes.

1. Introduction

Thermomechanical loads are present in many applications, and often represent a challenge for structures working in extreme environments. For example, this is the case of supersonic aircraft, which, in addition to mechanical loads, must endure the thermal loads inherent to high speed flight. Under such demanding conditions their lightweight design makes them highly susceptible to buckling. In order to preserve safety, efficiency and structural performance, understanding thermomechanical buckling becomes a key task.

Thermal buckling has been a topic of research since the early stages of supersonic flight, when the focus was on structures made of metallic materials. In the following decades, several research activities were conducted to investigate the thermal buckling of laminate composite materials. Whitney and Ashton [1] studied the effect of temperature and moisture in composite plates incorporating a generalized Duhamel-Neumann formulation, and assessed the buckling behaviour of generic, unsymmetric plates with all normal expansions restricted. Tauchert and Huang [2] extended this formulation for the study of thick antisymmetric laminate plates, incorporating Mindlin plate theory, solving the problem via the Galerkin method and assessing the effect of fixed and sliding boundary conditions. In later studies, Tauchert [3] particularized these studies into symmetric laminates using Rayleigh-Ritz method, while Sun and Hsu [4] developed a formula for thick, cross-ply, symmetric and balanced laminates using the Galerkin method. Meyers and Hyer [5] studied buckling and postbuckling of symmetric laminates, investigating the influence of the deviation of the load direction with respect to the material axis, using the Rayleigh-Ritz method. Abramovich [6] studied the buckling of cross-ply laminates under uniform thermal increment, considering a first-order shear deformation theory. Jones [7] investigated both unidirectional and cross-ply laminates under uniform heating and restricted normal expansions. It is especially remarkable the effort of Nemeth [8], who derived the buckling temperatures for an extensive range of long, fully restrained laminated plates. Matsunaga [9] developed 2D global higher-order deformation theory for thermal buckling of cross-ply laminated composite and sandwich plates. More recently, Vescovini et al. [10] developed a refined 2D model for generic panels (both sandwich and monolithic), able to selectively account for higher order theories in specific regions of interest. Li et al. conducted research on the effect of scatter in material properties [11] and on the effect of thermal gradients over the buckling temperature [12].

Thermal buckling has also been approached using finite element analysis: Shi et al. [13] studied thermal buckling and postbuckling of composite plates using the finite element modal coordinate method; Shiau et al. [14] assessed the influence of the lamina stiffness ratio E_L/E_T and lamina thermal expansion ratio α_2/α_1 in the buckling pattern formation of heated laminated plates using the finite element method. Ounis et al. [15] proposed a new type of finite element using a combination of linear isoparametric membrane element and a high precision rectangular Hermitian element.

However, most of mentioned analytical and numerical studies

* Corresponding author.
E-mail addresses: j.gutierrezalvarez@tudelft.nl (J. Gutiérrez Álvarez), c.bisagni@tudelft.nl (C. Bisagni).

https://doi.org/10.1016/j.compstruct.2019.111622
Received 20 May 2019; Received in revised form 10 October 2019; Accepted 28 October 2019
Available online 31 October 2019
0263-8223/

consider only thermal buckling, i.e. buckling caused merely by constrained thermal expansions, plate edges are kept straight and constant in length and the original dimensions of the panel remain unchanged. The influence of external mechanical loads in the buckling temperature and shape cannot be assessed unless plate size variation is incorporated in the formulation. Although in the last decade extensive analytical research has been done in the field of pure mechanical buckling [16–22], only few studies explore the buckling of mechanically and thermally loaded panels, like the one of Jones [23] for metallic materials, or Nemeth [24] for infinite laminate plates. Some authors like Noor et al. [25], or more recently Nali and Carrera [26], studied thermomechanical buckling using finite element models based on multilayered panel formulations.

This paper presents an analytical formulation for the calculation of buckling temperatures under the effect of external mechanical load and restrained transversal expansion. The analysis of symmetric and balanced composite laminated plates is presented, where temperature increment is applied and mechanical load is introduced in the form of shortening. Examples of plates made of different composite materials and different lay-ups are analysed and compared. The obtained formula can be used during initial design, for sensitivity analysis and also for deriving specific buckling shapes.

2. Problem formulation

A rectangular plate of length a and width b is considered. The plate is placed in a XYZ coordinate system, being the plane XY coincident with the mid-plane of the plate, and the Z axis perpendicular to this plane. In the present study two different types of boundary conditions are considered. The first type consists of plates that can experiment variations in length while their width remains unchanged. Plate edges are not allowed to displace out-of-plane. A graphical representation of the described constraints can be found in Fig. 1a, while the corresponding equations are presented below:

$$\begin{array}{lll} at\ \ X=0,a\text{:} & u^0=\pm\Delta_x/2 & at\ \ Y=0,b\text{:}\ \ u^0=free \\ & v^0=free & v^0=0 \\ & w^0=0 & w^0=0 \end{array}$$

where u^0, v^0, w^0 are the displacements of the plate mid-plane in the respective X, Y and Z directions. The plate is subjected to total length variations Δ_x along X axis. Positive values of Δ_x are taken for plate stretching, while plate shortening is assumed negative. The plate experiments an uniform temperature increment ΔT respect from a stress-free state. The order of load application is indifferent: ΔT can be applied before Δ_x, and also the other way around.

The second type of boundary conditions can be understood as a particular case of the first type. For this case, both plate length and width remain unchanged. The equations describing this new set of constraints can be easily achieved enforcing $\Delta_x = 0$ in the equations for the first type. The corresponding graphical representation is reported in Fig. 1b.

A plate under the first type of boundary conditions will now be considered. The plate is analysed by means of classical plate theory in combination with classical lamination theory (CLT). The laminate layup is assumed to be orthotropic, and material properties are considered to remain constant within the analysed range of temperatures.

The in-plane behaviour of the laminate is governed by the membrane constitutive equations (Eq. (1)):

$$\begin{Bmatrix} N_x \\ N_y \\ N_{xy} \end{Bmatrix} = \begin{bmatrix} A_{11} & A_{12} & 0 \\ A_{12} & A_{22} & 0 \\ 0 & 0 & A_{66} \end{bmatrix} \begin{Bmatrix} \epsilon^0_{xx} \\ \epsilon^0_{yy} \\ \gamma^0_{xy} \end{Bmatrix} - \begin{Bmatrix} N^T_x \\ N^T_y \\ N^T_{xy} \end{Bmatrix} \tag{1}$$

where N_x, N_y, N_{xy} are the force resultants at the plate edges, the terms A_{ij} $(i, j = 1, 2, 6)$ are the membrane stiffness terms from CLT,

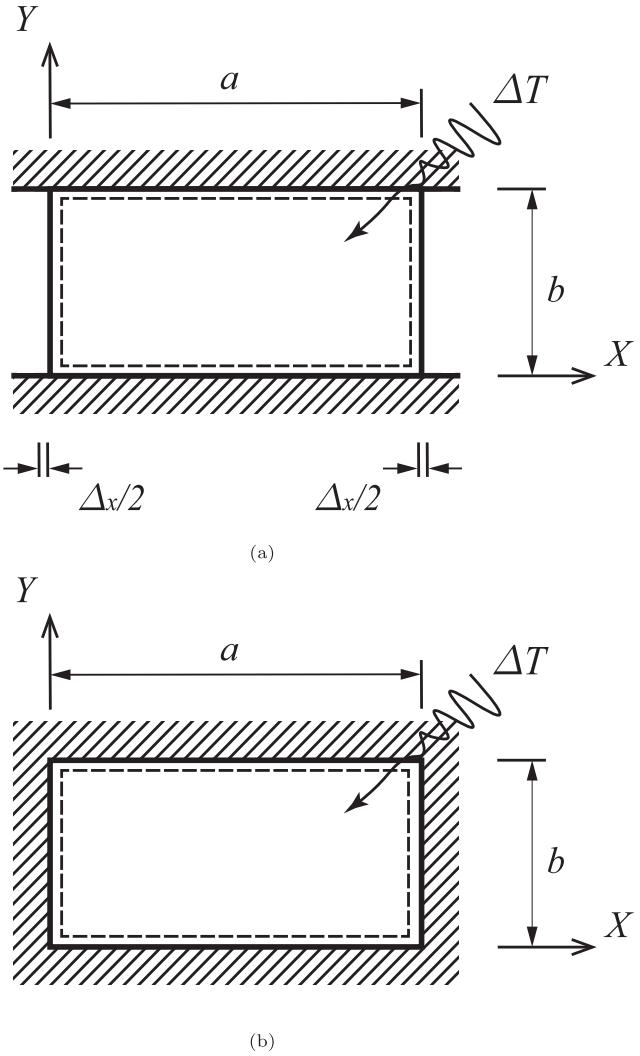

Fig. 1. Heated plates: (a) Plate with transversal expansion restrained and prescribed length variation. (b) Plate with all expansions restrained.

ϵ^0_{xx}, ϵ^0_{yy}, γ^0_{xy} are the engineering strains of the mid-plane of the plate, and N^T_x, N^T_y, N^T_{xy} are the thermal force resultants. The in-plane displacements can be described as linear functions of the total plate length variations Δ_x. The thermal force resultants are expressed as showed in Eq. (2):

$$\begin{Bmatrix} N^T_x \\ N^T_y \\ N^T_{xy} \end{Bmatrix} = \sum_{k=1}^{N} \int_{z_{k-1}}^{z_k} \begin{bmatrix} Q_{xx} & Q_{xy} & Q_{xs} \\ Q_{xy} & Q_{yy} & Q_{ys} \\ Q_{xs} & Q_{ys} & Q_{ss} \end{bmatrix} \begin{Bmatrix} \alpha^{(k)}_x \\ \alpha^{(k)}_y \\ \alpha^{(k)}_{xy} \end{Bmatrix} \Delta T dz \tag{2}$$

where Q_{ij} $(i, j = x, y, s)$ are the in-plane stiffnesses of a single lamina projected into XYZ coordinate system, k is a generic lamina number and N the total amount of laminae, and $\alpha^{(k)}_x$, $\alpha^{(k)}_y$, $\alpha^{(k)}_{xy}$ are the coefficients of thermal expansion (CTE) for a single lamina in the same coordinate system. Considering the temperature distribution homogeneous, the thermal force resultants are linear functions of ΔT, and can be expressed as in Eq. (3):

$$N^T_x = \widehat{N}^T_x \Delta T \qquad N^T_y = \widehat{N}^T_y \Delta T \qquad N^T_{xy} = \widehat{N}^T_{xy} \Delta T \tag{3}$$

where $\widehat{N}^T_x$, $\widehat{N}^T_y$, $\widehat{N}^T_{xy}$ are the thermal force resultants per unit thermal change. These quantities are function of lamina properties and stacking orientation. For symmetric and balanced laminates, $\widehat{N}^T_{xy}$ vanishes.

The membrane state is analysed considering linear displacements along the length and zero across the width, yielding Eq. (4), which are solution to the pre-buckling problem:

$$N_x = A_{11}\frac{\Delta_x}{a} - \widehat{N}_x^T \Delta T N_y = A_{12}\frac{\Delta_x}{a} - \widehat{N}_y^T \Delta T \tag{4}$$

being $N_{xy} = 0$. Eq. (4) represent the force resultants at the plate edges and constitute the membrane state of the loaded plate. They are functions of both Δ_x and ΔT.

The buckling equation is expressed by Eq. (5):

$$D_{11}w_{,xxxx} + 2(D_{12} + 2D_{66})w_{,xxyy} + D_{22}w_{,yyyy} - N_x w_{,xx} - N_y w_{,yy} = 0 \tag{5}$$

being the D_{ij} $(i, j = 1, 2, 6)$ the laminate bending stiffnesses, and meaning the comma in the subindex partial differentiation with respect to the indicated variable. A solution for Eq. (5) is now assumed. This solution has the form of double Fourier series, as presented in Eq. (6):

$$w = \sum_{m=1}^{\infty}\sum_{n=1}^{\infty} W_{mn}\sin\left(\frac{m\pi x}{a}\right)\sin\left(\frac{n\pi y}{b}\right) \tag{6}$$

where W_{mn} $(m, n = 1, 2, 3...)$ are the amplitudes of the Fourier series terms, and m and n represent the number of half-waves in X and Y directions. After substituting Eq. (6) for the out-of-plane displacements and Eq. (4) for the in-plane force resultants into Eqs. (5) and (7) appears:

$$\sum_{m=1}^{\infty}\sum_{n=1}^{\infty}\left(\frac{\pi^4(a^4n^4D_{22} + 2a^2b^2m^2n^2(D_{12} + 2D_{66}))}{a^4b^4} + + \frac{\pi^4b^4m^4D_{11}}{a^4b^4} - \frac{\pi^2(\widehat{N}_x^T ab^2m^2\Delta T + \widehat{N}_y^T a^3n^2\Delta T)}{a^3b^2} + -\frac{\pi^2(-(a^2n^2A_{12} - b^2m^2A_{11})\Delta_x)}{a^3b^2}\right)W_{mn}\sin\left(\frac{m\pi x}{a}\right)\sin\left(\frac{n\pi y}{b}\right) = 0 \tag{7}$$

After proper evaluation, the expression in Eq. (8) is obtained:

$$\Delta T = \frac{a^2n^2A_{12} + b^2m^2A_{11}}{b^2m^2\widehat{N}_x^T + a^2n^2\widehat{N}_y^T}\left(\frac{\Delta_x}{a}\right) + \frac{\pi^2(b^4m^4D_{11} + 2a^2b^2m^2n^2(D_{12} + 2D_{66}) + a^4n^4D_{22})}{a^2b^2\left(b^2m^2\widehat{N}_x^T + a^2n^2\widehat{N}_y^T\right)} \tag{8}$$

Eq. (8) represents the states of equilibrium for which the out-of-plane deflections are nonzero. For each state of equilibrium given by the number of half-waves m and n, the obtained Eq. (8) relates plate length variations Δ_x with thermal increments ΔT. For a certain value of Δ_x, the buckling temperature ΔT_{cr} is given by the buckling configuration (i.e. number of half-waves m and n) that delivers the lowest absolute value of ΔT. The presented deduction has been done using Δ_x as loading condition. A deduction using force resultants is also possible. However, it would introduce complexity as two types of force resultants, one mechanical and another thermal, would be necessary.

Eq. (8) has been deduced using simply supported boundary conditions. These are a simplification of reality and may not always capture the behaviour of the actual boundary conditions in a real structure.

3. Application cases

A few examples of heated composite plates are here presented. The plates are subjected to the two types of boundary conditions described in Section 2. The first set examples, reported in Section 3.1, deal with the case of fully restrained thermal expansions. Results in this section are given in the form of buckling charts, illustrating the change of ΔT_{cr} versus varying aspect ratio a/b. The second set of examples, presented in Section 3.2 correspond to the first type of boundary conditions, and cope with the case of simultaneous heating and external mechanical load. For this section, results are given in the form of buckling charts representing the variation of ΔT_{cr} versus applied Δ_x.

For all presented buckling charts, a few finite element analyses are performed in Abaqus for verification. In all diagrams, the results of the corresponding eigenvalue analyses are reported with the symbol of a circle. Buckling shapes obtained using Abaqus are also reported next to the corresponding buckling curve in the diagrams.

3.1. Buckling of heated, fully restrained plates

An orthotropic composite laminate plate is now considered. The plate has in-plane expansions along X and Y axis restrained, while it experiments a uniform temperature increment ΔT. The plate can buckle when a ΔT is applied. The equation for thermal buckling can be obtained from previously deduced Eq. (8). Considering that the plate does not experiment any length variation, $\Delta_x = 0$. Thus, Eq. (9) unfolds:

$$\Delta T = \frac{\pi^2(b^4m^4D_{11} + 2a^2b^2m^2n^2(D_{12} + 2D_{66}) + a^4n^4D_{22})}{a^2b^2(b^2m^2\widehat{N}_x^T + a^2n^2\widehat{N}_y^T)} \tag{9}$$

Eq. (9) gives the thermal buckling of thin, orthotropic, fully restrained composite laminated plates. For a certain plate geometry, material and stacking orientation, ΔT_{cr} is given by the buckling shape, i.e. values of m and n, delivering the minimal absolute value of ΔT. This equation has been already obtained in previous studies [4,2].

Some important features can be inferred from Eq. (9). For instance, the sign of the critical buckling temperature ΔT_{cr} can often be predicted by looking at the signs of $\widehat{N}_x^T$ and $\widehat{N}_y^T$. If both quantities are positive, plates buckle when heated; if both quantities are negative, plates buckle when cooled down. However, when quantities $\widehat{N}_x^T$ and $\widehat{N}_y^T$ have opposite sign, plates may buckle either when heated, cooled down, or under both conditions simultaneously. This particular phenomenon can be easily clarified: for a given plate geometry, layup and material, the numerator in Eq. (9) is always positive, because it merely depends on plate geometry and bending stiffness; however, the denominator may have positive and negative values due to $\widehat{N}_x^T$ and $\widehat{N}_y^T$, ultimately affecting to the sign of ΔT_{cr}.

Eq. (9) can also be easily related to an equivalent formula for metallic materials. In terms of material behaviour, isotropy could be seen as a particular case of orthotropy. In order to perform such conversion, the following equivalences have to be considered: $D_{11} = D_{22} = D_{12} + 2D_{66} = D$, $A_{12}/A_{11} = \nu$, $\widehat{N}_x^T = \widehat{N}_y^T = \widehat{N}^T$. Plugging $= Eh\alpha\Delta T/(1-\nu)$ these in Eqs. (9) and (10) unfolds:

$$\Delta T = \frac{\pi^2(1-\nu)D}{Eh\alpha}\left(\frac{m^2}{a^2} + \frac{n^2}{b^2}\right) \tag{10}$$

where ν is the isotropic Poisson ratio, α the CTE for isotropic materials, and D the plate bending stiffness from classical plate theory. It is possible to note that isotropic materials, ΔT_{cr} is always reached for $m = n = 1$ configurations. Thus, Eq. (10) is the formula for thermal buckling of thin, fully restrained isotropic plates. Eq. (10) has been previously documented in literature [27,28].

Eq. (9) is at first verified against results extracted from literature ([13–15]). The aim of this verification is establishing the range of applicability of Eq. (9). The three chosen bibliographic sources analyse the same benchmark case, consisting in simply supported, fully restrained composite laminated plates of dimensions $381 \times 304 \times 1.22$ mm^3, made of composite material with following ply properties: $E_1 = 155$ GPa, $E_2 = 8.07$ GPa, $G_{LT} = 4.55$ GPa, $\nu_{LT} = 0.22$, $\alpha_1 = -0.07\cdot10^{-6}/°C$, $\alpha_2 = 30.1\cdot10^{-6}/°C$, and stacking sequences $[0/90/90/0]_s$ and $[0/45/-45/90]_s$. These plates are also analysed applying Eq. (9) and performing finite element analysis using Abaqus. For the Abaqus numerical analysis, plates were modelled as rectangular geometries, meshed with rectangular S4R shell elements, with an element size of approximately 25 mm. The results of these verifications are presented in Table 1.

The first row of Table 1 corresponds to a $[0/90/90/0]_s$ layup. It is a specially orthotropic laminate. The value delivered by Eq. (9) is in very

Table 1
Verification of buckling temperatures with different composite plates.

Stacking	Eq. (9) [°C]	Abaqus [°C]	Shi [13] [°C]	Shiau [14] [°C]	Ounis [15] [°C]
$[0/90/90/0]_s$	6.81	6.86	6.81	6.81	6.81
$[0/45/-45/90]_s$	7.86	7.67	7.62	7.65	7.63

good agreement with the values extracted from literature, while the result delivered by Abaqus is slightly larger, approaching to the exact value delivered by Eq. (9) from the stiffer side. The results in the second row of Table 1 correspond to the $[45/-45/0/90]_s$ quasi-isotropic stacking sequence. In this case, the terms D_{16} and D_{26} are nonzero, so using Eq. (9) can be considered as an approximation. The value delivered by Eq. (9) is a bit higher than both Abaqus and literature values. This is due to the non-negligible contribution of the bending anisotropy terms.

Three examples of composite laminate plates are now analysed and discussed.

The first example studies plates of variable length and constant plate width $b = 375$ mm. The plates have quasi-isotropic stacking sequence $[45/-45/0/90]_{2s}$, and are made of *AS4*/3502 composite material. Material properties are reported in Table 2. For this combination of layup and material, both laminate CTE's α_x and α_y, as well as quantities N_x^T and N_y^T are positive. The bending-twisting coupling terms are non-zero. However, being the ratio D_{16}/D_{22} a 7%, the influence of bending anisotropy over the solution is negligible. These quantities are reported in Table 3. The output of Eq. (9) are plotted in Fig. 2, in the form of a chart representing applied ΔT versus varying aspect ratio a/b. For instance, takings $n = 1$ and $m = 1, 2, 3...$, a set of dashed lines are generated, each one of them corresponding to buckling shapes of increasing number of half-waves along X direction; by repeating this operation with $m = 1$, $n = 1, 2, 3$, curves related to shapes with multiple half-waves in Y direction are obtained. For a certain value of the aspect ratio, ΔT_{cr} is given by the dashed curve delivering the minimal absolute value of ΔT. The buckling curve is obtained by gathering together all values of ΔT_{cr}, and is represented as bold in Fig. 2. A characteristic feature of quasi-isotropic laminated plates can be noted: under the case of pure thermal buckling, quasi-isotropic plates tend to buckle in a single half-wave shape in both X and Y directions, independent of plate geometry. For increasing values of the aspect ratio, ΔT_{cr} rapidly decreases and tends asymptotically to a stable value.

For very large values of a/b, the critical temperature ΔT_{cr} tends to $\Delta T_{cr,\infty}$, which is the critical buckling temperature for simply supported, fully restrained, heated infinite plates, reported also in literature [8]. Such temperature has been reported as dash-dotted line in Fig. 2. This trend is also observed in heated, simple supported, fully restrained metallic plates.

The second example presents buckling temperatures for plates having identical geometry and stacking orientation as in previous example. However, plates are now made of *IM*7/8552 composite material. For this new combination of layup and material, parameters α_x, α_y, N_x^T and N_y^T are negative, as reported in Table 3; as a direct consequence ΔT_{cr} will also be negative. As for previous example, the bending-twisting coupling terms are small in comparison with the rest of their bending stiffness terms, with a maximal ratio of 7%, the influence of bending anisotropy over the solution is negligible. The results delivered by Eq. (9) for this second example are presented in Fig. 3, in the form of a chart representing the change of ΔT versus a/b.

The curve of ΔT_{cr} for the current set of analysed plates shows similarities with the first analysed set of plates. Plates still buckle under a unique half-wave. However, laminate CTE's are negative due to the change of plate material, so plates now buckle under cooling and the resulting buckling chart appears as mirrored with respect from its *AS4*/3502 counterpart. Quasi-isotropic laminates with negative thermal expansion keep similar mechanical properties to isotropic materials, while their thermal buckling behaviour is reversed. For very long values of a/b, the critical temperature tends to $\Delta T_{cr,\infty}$, which is the critical temperature for simply supported, fully restrained, heated infinite plates reported in literature [8]. Composite laminate plates with negative thermal expansion are a consequence of either $\alpha_1^{(k)}$ and $\alpha_2^{(k)}$ lamina CTE's being negative, but also due to Poisson effect due to high fibre stiffness [1]. Such lamina properties can be used for tailoring stacking sequences with negligible or even zero thermal expansion.

The third example corresponds to plates sharing geometries with the two previous examples. Material remains *IM*7/8552 while the layup is now $[20/-20]_{4s}$. Contrary to previously analysed quasi-isotropic laminates, this stacking sequence shows higher membrane and bending stiffness along one prevalent direction. Additionally, the present combination of material and layup shows opposite signs for $\widehat{N}_x^T$ and $\widehat{N}_y^T$, as reported in Table 3. Layup is now angle-ply, so the bending-twisting coupling terms become proportionally larger. However, as shown in Ref. [29], the influence of bending anisotropy becomes smaller when the amount of layers increases. Thus, the formula can still be used for pre-sizing. As a consequence of this, plates may buckle either under heating, cooling, or both. The outcome of Eq. (9) is plotted in Fig. 4, following the same procedure used for Figs. 2 and 3. Two buckling curves appear, corresponding to both positive and negative ranges of ΔT. Thus, a certain plate can have two buckling temperatures. For instance, a plate with aspect ratio $a/b = 2.2$ will buckle under $\Delta T = 23.93$ °C with shape (1, 2), but also under $\Delta T = -10.47$ °C with shape (2, 1). The two buckling curves show opposing trends regarding the buckling shapes: for the positive range of ΔT, increasing values of a/b cause the number of half-waves along Y axis to decrease. Conversely, for negative range of ΔT, the number of half-waves increases along X axis. It is possible to note that half waves along a certain plate axis are a clear indicator of main compressive direction.

Angle-ply laminates showing high stiffness along one predominant direction can be useful when the loads are highly directional. These stacking orientations are often the output of optimization processes, where the fibres align to respond to critical loading directions. However, the direction perpendicular to the main fibre orientation is less stiff due to the lack of fibres, and it also sees much higher thermal expansion due to the larger contribution of the matrix material. This makes them prone to buckling when expansions along this direction are somewhat restrained. Potential applications in thermal environments should be considered carefully, especially if negative laminate CTE's are present as behaviour becomes more counter intuitive.

3.2. Buckling of loaded and heated plates

An orthotropic composite laminate plate is now considered. Its edges are simply supported, and the plate experiments an uniform length variation Δ_x along X axis, while the width remains constant. The plate is also subjected to a spatially uniform temperature increment ΔT. Under such situation, the plate can buckle either when a ΔT is applied, a Δ_x is applied, or both take place simultaneously. The described

Table 2
Material properties [24,33].

Material	E_{11} [GPa]	E_{22} [GPa]	G_{12} [GPa]	ν_{12}[−]	$\alpha_1 \cdot 10^6$[1/°C]	$\alpha_2 \cdot 10^6$ [1/°C]	t_{Ply} [mm]
AS4/3502	127.6	11.3	6.0	0.3	0.45	29.6	0.127
IM7/8552	150	9.08	5.29	0.32	−5.5	25.8	0.127

Table 3
Laminate CTE α_x and α_y, and thermal forces $\widehat{N}_x^T$ and $\widehat{N}_y^T$, for different materials and layups.

Material	Stacking	$\alpha_x \cdot 10^6$[1/°C]	$\alpha_y \cdot 10^6$[1/°C]	$\widehat{N}_x^T$ [N/mm °C]	$\widehat{N}_y^T$ [N/mm °C]
*AS*4/3502	$[45/-45/0/90]_{2s}$	3.35	3.35	0.49	0.49
*IM*7/8552	$[45/-45/0/90]_{2s}$	−3.23	−3.23	−0.54	−0.54
*IM*7/8552	$[20/-20]_{4s}$	−8.09	20.07	−1.30	0.21

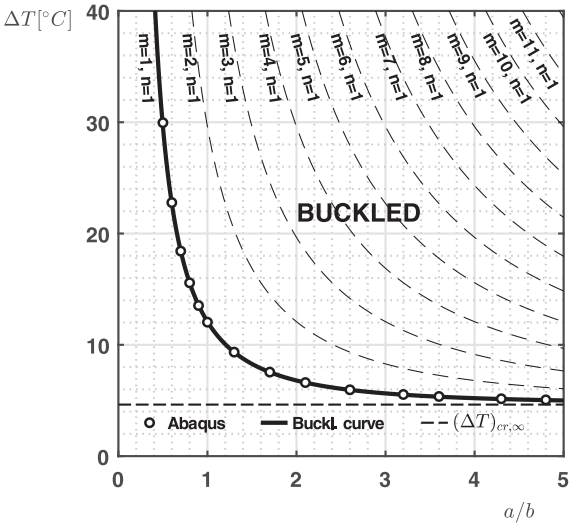

Fig. 2. Buckling temperatures of fully restrained, heated composite plates with different lengths. Material: *AS*4/3502; Layup: $[45/-45/0/90]_{2s}$.

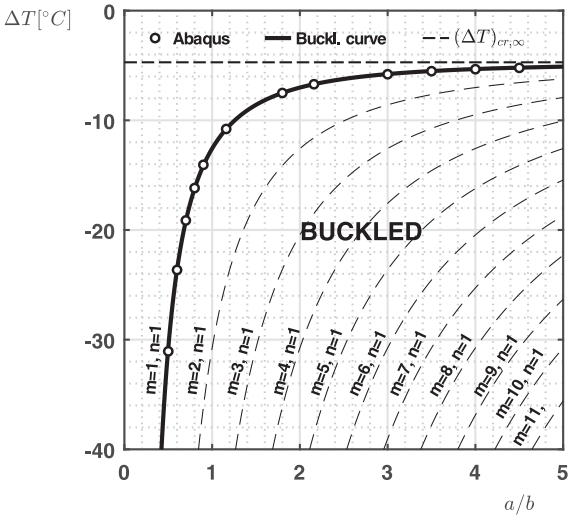

Fig. 3. Buckling temperatures of fully restrained, heated composite plates with different lengths. Material: *IM*7/8552; Layup: $[45/-45/0/90]_{2s}$.

situation corresponds to the first type of boundary conditions specified in Section 2. For these plate and loading conditions, Eq. (8) holds.

There are some substantial differences between Eqs. (8) and (9). For instance, when the plate is subjected to a prescribed Δ_x, the temperature is a linear function of mechanical loading condition Δ_x. As a consequence, the load proportionality ratio $k = N_x/N_y$ no more remains constant, and the sign of ΔT_{cr} does not depend only on plate properties anymore.

Eq. (8) can be related to a formula for isotropic materials, as done previously with Eq. (9). Thus, after introducing in Eq. (8) the equivalences for isotropic material and doing proper rearrangements, Eq. (11) unfolds:

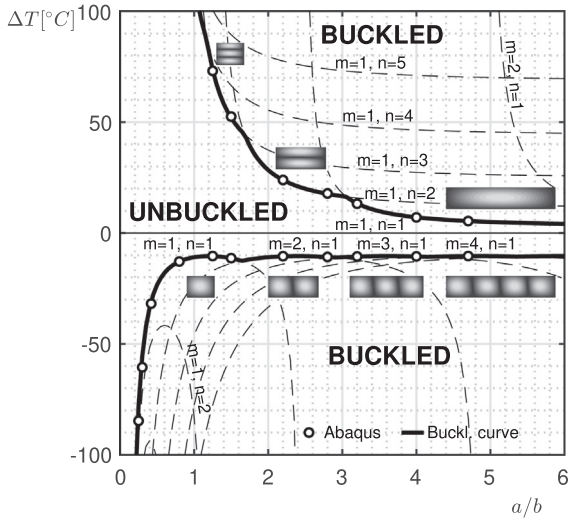

Fig. 4. Buckling temperatures of fully restrained, heated composite plates with different lengths. Material: *IM*7/8552; Layup $[20/-20]_{4s}$.

$$\frac{E\alpha h b^2}{\pi^2 D}\Delta T = \frac{a^2 b^2 n^2 \nu + b^4 m^2}{a^2 n^2 \pi^2 D} N_x + \frac{(a^2 n^2 + b^2 m^2)^2}{a^4 n^2} \tag{11}$$

Eq. (11) is the equation for thermomechanical buckling in isotropic materials, reported in literature [7].

Three examples are then presented and discussed, analysing three different thermomechanically loaded composite laminate plates. The three analysed plates present the same plate width b, layup and material of the three set of plates analysed in Section 3.1, so examples in both sections can easily be related to each other. In all cases, plates are very thin in comparison to their length and width, which is unrealistic in real applications. Such choice of dimensions has been made so that obtained buckling temperatures are small, and can be applied easily during tests.

The first analysed plate is made of *AS*4/3502 material, with a quasi-isotropic stacking sequence $[45/-45/0/90]_{2s}$, width $b = 375$ mm and length $a = 575$ mm. As stated in previous Section 3.1, for this combination of stacking and material, the quantities α_x, α_y, N_x^T and N_y^T are positive.

Results from Eq. (8), are plotted in a buckling chart representing ΔT versus Δ_x. Starting from a buckling shape with $m = 1$, $n = 1$ a line is obtained by plotting the resulting expression and is represented as dashed in Fig. 5. By leaving now n = 1 fixed, and assuming $m = 1, 2, 3, \ldots$, analogue dashed lines can be generated, being these lines related to buckling shapes with multiple half-waves in X direction. By taking $m = 1$, $n = 1, 2, 3, \ldots$similar dashed lines related to buckling shapes with multiple half-waves in Y direction are reported. For a certain length variation Δ_x, the critical buckling temperature ΔT_{cr} is determined by the dashed line delivering the lowest absolute value of ΔT. These lines intersect each other so the buckling shape defining the lowest ΔT will change depending on the mechanical loading condition Δ_x. The result of collecting all values of ΔT_{cr} for any given Δ_x is the buckling curve, represented as bold in Fig. 5, and is constituted by different segments of several intersecting dashed lines.

The buckling curve divides the loading plane $(\Delta_x, \Delta T)$ into two

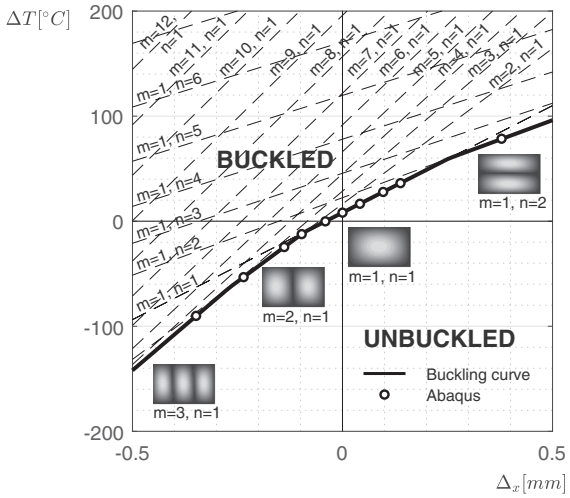

Fig. 5. Buckling chart for a loaded and heated composite plate. Geometry: $a = 575$ mm, $b = 375$ mm; Material: $AS4/3502$; Layup: $[45/-45/0/90]_{2s}$.

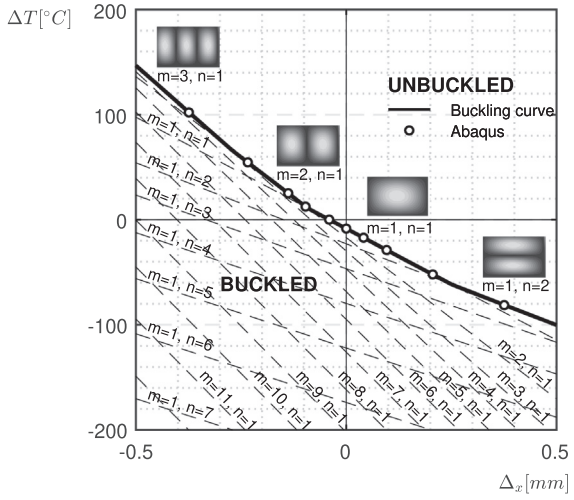

Fig. 6. Buckling chart for a loaded and heated composite plate. Geometry: $a = 575$ mm, $b = 375$ mm; Material: $IM7/8552$; Layup: $[45/-45/0/90]_{2s}$.

subspaces, corresponding to buckled and unbuckled states. The intersection of the buckling curve with the horizontal axis corresponds to the loading situation in which the plate buckles under pure mechanical loading ($\Delta T = 0$ °C); for this case, the length variation has a value of $\Delta_x = -0.04$ mm and the plate buckles under the shape of one half-wave in both X and Y directions. Conversely, the intersection with the vertical axis represents the case in which $\Delta_x = 0$ mm and buckles under pure heating. For this case, the plate buckles under $\Delta T_{cr} = 8.14$ °C, and this value can be found also in Fig. 2. The buckling shape has only one half-wave in both X and Y directions.

In the case that the plate experiments a stretch of $\Delta_x = 0.3$ mm, ΔT_{cr} increases significantly, rising up to 66.62 °C and the buckling presents a mode with two half waves in Y direction. It is possible to note that under heating conditions, plate stretching has stabilizing effect against buckling. States of stretching and cooling induce biaxial tension states in the plate so buckling under this loading condition is not possible. Conversely, if the plate experiments a shortening of $\Delta_x = -0.02$ mm, ΔT_{cr} descends to 3.06 °C. Under states of shortening and heating, the plate experiments a state of biaxial compression that noticeably reduces ΔT_{cr}. Considering now a shortening of $\Delta_x = -0.3$ mm, that is larger than the critical shortening for pure mechanical loading. In order to prevent buckling, the plate should be cooled down to temperatures lower than $\Delta T_{cr} = -73.74$ °C. In this case, the buckling pattern corresponds to three half-waves in the axial direction.

It can be stated that the increase of mechanical condition Δ_x induces a change in the buckling temperature ΔT_{cr}, as well as variations in the direction and number of half waves. The buckling behaviour of quasi-isotropic plates under thermomechanical loads is, therefore, comparable to that one shown by metallic plates [7].

The second analysed plate shares dimensions and quasi-isotropic layup with the previously analysed plate; the only difference between the two plates is the material, which is now $IM7/8552$. The resulting buckling chart is presented in Fig. 6, and is generated with the same procedure used for Fig. 5. The new buckling chart appears as mirrored with respect to the horizontal axis when compared to its $AS4/3502$ counterpart. This is a consequence of the variation in sign of quantities α_x, α_y, N_x^T, N_y^T, caused by the material $IM7/8552$. The consequences of such inversion is that plate stretching has now a stabilizing effect against cooling, and under plate compression, a positive ΔT is required in order to prevent buckling. The mechanical condition Δ_x induces a change in the buckling temperature ΔT_{cr}, as well as variations in the direction and number of half waves. Laminates with negative CTE's show a counter-intuitive behaviour when external mechanical load is present. This should be taken into account when considering them for

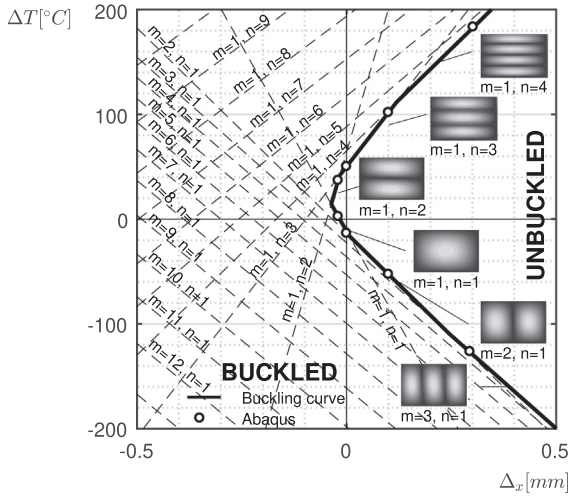

Fig. 7. Buckling chart for a loaded and heated composite plate. Geometry: $a = 575$ mm, $b = 375$ mm; Material: $IM7/8552$; stacking: $[20/-20]_{4s}$.

any application involving notable changes in temperature.

The third analysed plate is made of $IM7/8552$ and the stacking is $[20/-20]_{4s}$. A new buckling chart, Fig. 7, is generated. For this combination of material and laminate stacking, N_x^T and N_y^T have opposite sign. In this case, with a stretching equal to $\Delta_x = 0.1$ mm, the plate buckles under $\Delta T_{cr} = 101.8$ °C, with a (1,3) buckling shape, but also under $\Delta T_{cr} = -52.62$ °C. It is also possible to note that the graph is not symmetric with respect to X axis. For heating, the plate buckles in a pattern of increasing half-waves in transversal direction Y, while for cooling in increasing number of half-waves along X direction. It is also remarkable to see how the area for negative Δ_x area experiments a substantial reduction, and neither heating nor cooling have a proper stabilizing effect against buckling when mechanical load is compressive. This kind of information can be valuable when considering the suitability of highly directional laminates for thermomechanically loaded environments.

Throughout the last three examples, it has been shown how the introduction of heat and external load, combined with restrained transversal expansions affects the buckling behaviour of some frequently used families of composite laminated plates. For structural applications in extreme environments, buckling loads experience dramatic changes when thermal increments are present. Such interaction effects should be properly contemplated early on in the sizing phases, and can be also used for obtaining desired buckling shapes.

There are other factors related to materials or manufacturing, which have not been addressed and are well worth considering. One of them is the effect of thermal pre-stress due to curing on buckling loads [30]: often plates and longitudinal stiffeners have different CTE's, creating in this way residual stresses that can have an impact on the buckling load. Another relevant factor is the temperature dependence on material characteristics: Temperature variation may induce changes on properties, making buckling temperatures differ from those predicted using material values at room temperature. Such variations are strongly dependent on the material of choice. It remains the task of the design engineer to perform a thorough research on the behaviour of any potential material within the desired range of temperatures. For example, some carbon/epoxy composite materials show an increase on longitudinal lamina stiffness within − 50 °C and − 200 °C range, as documented in Ref. [31]; Nonlinear dependence of thermal expansion on temperature has been registered in various materials, as reported in Ref. [32].

4. Conclusions

The buckling of orthotropic laminated plates under heating, restrained transversal expansion and external mechanical load in axial direction was investigated.

A closed formula was deduced and compared against the classical thermal buckling problem with no plate size variation. Different sets of results in graphical form for both mentioned loading cases were presented and compared. Resulting buckling charts show buckling curves that divide the displacement-temperature loading space into two subspaces, corresponding to buckled and unbuckled states. The influence of external mechanical load over the plate buckling temperature (and vice versa) was assessed. It was shown that mechanically loaded laminated plates can be either stabilized or destabilized by either cooling or heating. Besides, it was also shown how the combination of heating and mechanical load have an impact on the buckling shape, so under specific loading conditions desired plate shapes can be targeted. The proposed formula, due to its simplicity, can readily be used for initial design, sensitivity analysis or optimization.

Declaration of Competing Interest

The authors declare that they have no known competing financial interests or personal relationships that could have appeared to influence the work reported in this paper.

Appendix A. Supplementary data

Supplementary data associated with this article can be found, in the online version, athttps://doi.org/10.1016/j.compstruct.2019.111622.

References

[1] Whitney J, Ashton J. Effect of environment on the elastic response of layered composite plates. AIAA J 1971;9(9):1708–13. https://doi.org/10.2514/3.49976.

[2] Tauchert TR. Thermal buckling of thick antisymmetric angle-ply laminates. J Therm Stresses 1987;10(2):113–24. https://doi.org/10.1080/01495738708927000.

[3] Tauchert TR, Huang NN. Thermal buckling of symmetric angle-ply laminated plates. Compos Struct 1987;4:424–35 URL: http://link.springer.com/chapter/10.1007/978-94-009-3455-9_33.

[4] Sun LX, Hsu TR. Thermal buckling of laminated composite plates with transverse shear deformation. Comput Struct 1990;36(5):883–9. https://doi.org/10.1016/0045-7949(90)90159-Y. URL: http://www.sciencedirect.com/science/article/pii/004579499090159Y.

[5] Meyers CA, Hyer MW. Thermal buckling and postbuckling of symmetrically laminated composite plates. J Therm Stresses 1991;14(4):519–40. https://doi.org/10.1080/01495739108927083.

[6] Abramovich H. Thermal buckling of cross-ply composite laminates using a first-order shear deformation theory. Compos Struct 1994;28:201–13. URL: http://www.sciencedirect.com/science/article/pii/0263822394900493.

[7] Jones RM. Thermal buckling of uniformly heated unidirectional and symmetric cross-ply laminated fiber-reinforced composite uniaxial in-plane restrained simply supported rectangular plates, Composites Part A: Applied Science and Manufacturing 36 (10 Spec. Compos Part A: Appl Sci Manuf 2005;36(10 Spec. Iss.):1355–67. https://doi.org/10.1016/j.compositesa.2005.01.028.

[8] Nemeth MP. Buckling behavior of long anisotropic plates subjected to fully restrained thermal expansion, Tp-2003-212131. Natl Aeronaut Space Administration 2003. URL: http://hdl.handle.net/2060/19970004648.

[9] Matsunaga H. Thermal buckling of cross-ply laminated composite and sandwich plates according to a global higher-order deformation theory. Compos Struct 2005;68(4):439–54. https://doi.org/10.1016/j.compstruct.2004.04.010.

[10] Vescovini R, D'Ottavio M, Dozio L, Polit O. Thermal buckling response of laminated and sandwich plates using refined 2-D models. Compos Struct 2017;176(2017):313–28. https://doi.org/10.1016/j.compstruct.2017.05.021.

[11] Li J, Tian X, Han Z, Narita Y. Stochastic thermal buckling analysis of laminated plates using perturbation technique. Compos Struct 2016;139(2016):1–12. https://doi.org/10.1016/j.compstruct.2015.11.076.

[12] Li J, Narita Y, Wang Z. The effects of non-uniform temperature distribution and locally distributed anisotropic properties on thermal buckling of laminated panels. Compos Struct 2015;119(2015):610–9. https://doi.org/10.1016/j.compstruct.2014.09.011.

[13] Shi Y, Lee RY, Mei C. Thermal postbuckling of composite plates using the finite element modal coordinate method. J Therm Stresses 1999;22(6):595–614. https://doi.org/10.1080/014957399280779.

[14] Shiau LC, Kuo SY, Chen CY. Thermal buckling behavior of composite laminated plates. Compos Struct 2010;92(2):508–14. https://doi.org/10.1016/j.compstruct.2009.08.035.

[15] Ounis H, Tati A, Benchabane A. Thermal buckling behavior of laminated composite plates: a finite-element study. Front Mech Eng 2014;9(1):41–9. https://doi.org/10.1007/s11465-014-0284-z.

[16] Bisagni C, Vescovini R. Fast tool for buckling analysis and optimization of stiffened panels. J Aircraft 2009;46(6):2041–53. https://doi.org/10.2514/1.43396.

[17] Bisagni C, Vescovini R. Analytical formulation for local buckling and post-buckling analysis of stiffened laminated panels. Thin-Walled Struct 2009;47(3):318–34. https://doi.org/10.1016/j.tws.2008.07.006.

[18] Bisagni C, Vescovini R, Davila CG. Single-stringer compression specimen for the assessment of damage tolerance of postbuckled structures. J Aircr 2011;48(2):495–502.

[19] Weaver PM, Nemeth MP. Improved design formulas for buckling of orthotropic plates under combined loading. AIAA J 2008;46(9):2391–6. https://doi.org/10.2514/1.37892.

[20] Vescovini R, Bisagni C. Two-step procedure for fast post-buckling analysis of composite stiffened panels. Comput Struct 2013;128(2013):38–47. https://doi.org/10.1016/j.compstruc.2013.06.002.

[21] Vescovini R, Bisagni C. A fast procedure for the design of composite stiffened panels. Aeronaut J 2015;119(1212):185–201.

[22] Abramovich H, Bisagni C. Behavior of curved laminated composite panels and shells under axial compression. Prog Aerosp Sci 2015;78(2015):74–106. https://doi.org/10.1016/j.paerosci.2015.05.008.

[23] Jones R. Buckling of Bars, Plates, and Shells, Bull Ridge Corporation, Blacksburg, Va., 2006; 2006.

[24] Nemeth MP. Buckling behavior of long anisotropic plates subjected to restrained thermal expansion and mechanical loads. J Therm Stresses 2000;23(9):873–916. https://doi.org/10.1080/014957300750040122.

[25] Noor AK, Starnes JH, Peters JM. Thermomechanical buckling and postbuckling of multilayered composite panels. Compos Struct 1993;23(3):233–51. https://doi.org/10.1016/0263-8223(93)90225-F.

[26] Nali P, Carrera E. Accurate buckling analysis of composite layered plates with combined thermal and mechanical loadings. J Therm Stresses 2013;5739(January 2015):37–41. https://doi.org/10.1080/01495739.2012.663679. URL: http://www.tandfonline.com/doi/abs/10.1080/01495739.2012.663679.

[27] Boley B, Weiner J. Theory of Thermal Stresses 1960. New York: Wiley; 1960.

[28] Thornton EA. Thermal Structures for Aerospace Applications, Aiaa Education Series. American Institute of Aeronautics and Astronautics; 1996. https://doi.org/10.2514/4.862540. arXiv:arXiv:1011.1669v3, URL: https://arc.aiaa.org/doi/book/10.2514/4.862540.

[29] Nemeth MP. Importance of anisotropy on buckling of compression-loaded symmetric composite plates. AIAA J 1986;24(11):1831–5. https://doi.org/10.2514/3.9531.

[30] Müller de Almeida SF, Hansen JS. Enhanced elastic buckling loads of composite plates with tailored thermal residual stresses. J Appl Mech 1997;64(4):772. https://doi.org/10.1115/1.2788981.

[31] Kim MG, Kang SG, Kim CG, Kong CW. Tensile response of graphite/epoxy composites at low temperatures. Compos Struct 2007;79(1):84–9. https://doi.org/10.1016/j.compstruct.2005.11.031.

[32] Reed RP, Golda M. Cryogenic properties of unidirectional composites. Cryogenics 1994;34(11):909–28. https://doi.org/10.1016/0011-2275(94)90077-9.

[33] Camanho PP, Maimi P, Dávila CG. Prediction of size effects in notched laminates using continuum damage mechanics. Compos Sci Technol 2007;67(13):2715–27. https://doi.org/10.1016/j.compscitech.2007.02.005.